SIMULATION AND OPTIMIZATION METHODS FOR ASSESSING THE IMPACT OF AVIATION OPERATIONS ON THE ENVIRONMENT

Banavar Sridhar*, Neil Chen*, Hok K. Ng**
***NASA Ames Research Center, Moffett Field, CA 94035-1000**
****University of California, Santa Cruz@Moffet Field**
Keywords: *Aviation operations, Environmental impact, Simulation and optimization, Contrails, Models*

Abstract

There is increased awareness of anthropogenic factors affecting climate change and urgency to slow the negative impact. Greenhouse gases, oxides of Nitrogen and contrails resulting from aviation affect the climate in different and uncertain ways. This paper develops a flexible simulation and optimization software architecture to study the trade-offs involved in reducing emissions. The software environment is used to conduct analysis of two approaches for avoiding contrails using the concepts of contrail frequency index and optimal avoidance trajectories.

1 Introduction

There is increased awareness of anthropogenic factors affecting climate change and urgency to slow the negative impact [1,2]. Aviation operations affect the climate in several ways. CO_2, water vapor and other greenhouse gases are unavoidable by-product of the combustion of fossil fuel. The majority of the water vapor in the atmosphere is due to the evaporation of water. Transportation consumed 28% of the energy used in the US during 2008. It is estimated that aviation is responsible for 13% of transportation-related fossil fuel consumption and 2% of all anthropogenic CO_2 emissions. The emission of water vapor from the aircraft is small and may be of concern at higher altitudes. Nitric oxide and nitrogen oxide, commonly referred to as NO_x, created by the high temperatures in the aircraft engines affect the environment indirectly by affecting the distributions of ozone and methane. Contrails appear in the atmosphere along the aircraft trajectory at higher altitudes if the location has the right atmospheric conditions. Persistent contrails appear if the relative humidity with respect to ice is greater than 100%. There is a large uncertainty in the understanding of the impact of aviation on climate change. However, this uncertainty is bigger in the case of contrails as they have both negative and positive effects and the resulting net effect is a difference between large error prone estimates of similar magnitude. It is suggested that emissions at cruise altitudes may have a larger impact than emissions on the surface. Expert panels have suggested focusing on the impacts of subsonic aviation emissions at cruise altitudes in the upper troposphere and lower stratosphere [2]. It is likely that international treaties and legislation may lead to changes in aircraft operations.

The complexity and uncertainty in the understanding of the various components of the climate equation requires models, analysis, optimization and validation at several levels. This paper develops a flexible air traffic simulation and optimization toolbox with fuel, emission and contrails models to develop the data needed by policy-makers to make acceptable aviation operation decisions.

Section 2 describes the FACET air traffic simulation software and the interaction between simulation and optimization tools. Section 3 provides a brief description of the models for aircraft, wind, fuel flow, emissions, and contrail formation. It introduces a Contrail Frequency Index (CFI), a measure of severity of contrail formation based on nominal air traffic flow.

Section 4 discusses the issues involved in contrails avoidance, describes two avoidance approaches and preliminary results with one involving only altitude changes and another based on three-dimensional optimal trajectories. Section 5 provides some concluding remarks.

2 Simulation and Optimization Environment

2.1 Future Air Traffic Management Concepts Evaluation Tool (FACET)

FACET is a flexible software-based simulation environment for exploration, development, and evaluation of advanced Air Traffic Management (ATM) concepts [3]. FACET models system-wide airspace operations over the contiguous United States. Airspace models (e.g., Center/sector boundaries, airways, locations of navigation aids and airports) are available from databases. Weather models (winds, temperature, severe weather cells, etc.) are also available. FACET models aircraft trajectories using spherical-earth equations. The aircraft can be flown along their routes as they climb, cruise, and descend according to their individual aircraft-type performance models. FACET software consists of four components: 1) algorithms, 2) databases, 3) graphical user interface (GUI), and, 4) applications. The algorithms use data from the databases and process the information needed by the applications, where each application supports one or many ATM concepts. The applications generate decision support data, which are displayed on the GUI. Unique features include simulation of air traffic over North America, traffic forecasting, data visualization, and playback of recorded data. Real-time aircraft position data and flight plan data are obtained from the FAA's Enhanced Traffic Management System traffic data feed; wind and temperature data are obtained from the National Oceanic and Atmospheric Administration's (NOAA) weather data feed. The data from the static databases and dynamic data feeds are used for parsing the flight plan route and constructing four-dimensional (4D) trajectories for the climb, cruise, and descent phases of flight according to the performance characteristics of the individual aircraft type. These 4D trajectories provide the engine that drives various ATM applications. FACET also provides extensive two and three dimensional visualization capabilities for display of data generated by various applications. The FACET GUI binds algorithms, databases, applications and visualization tools together. The software, data and visualization components interact with each other via drop-down menus available in the GUI.

2.2 Modifications to FACET

An Application Programming Interface (API) enables FACET to interface with analytical tools in MATLAB® and large-scale optimization software such as CPLEX®. The FACET software together with the API has been used to develop efficient traffic flow management algorithms [4-5]. The FACET software has been further modified by the addition of contrails, fuel flow and emission models as shown in Fig. 1.

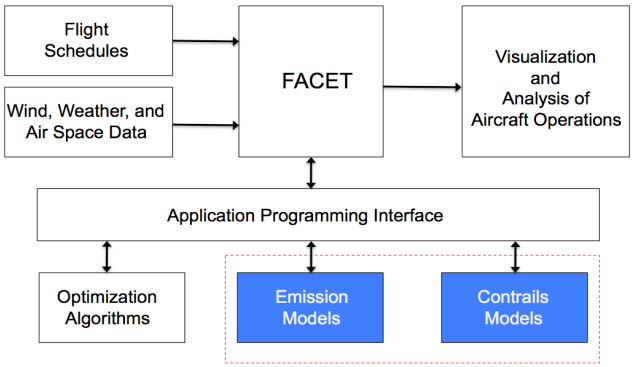

Fig 1. FACET interaction with optimization, emission and contrail models.

3 Models

3.1 Aircraft

Aircraft are modeled as 3-dimensional point mass using an inertial reference system. The values of the parameters vary depending on the aircraft. The equations of motion can be defined by the equations:

$$
\begin{aligned}
\dot{x} &= V\cos\varphi\cos\gamma + u(x,y) \\
\dot{y} &= V\sin\varphi\cos\gamma + v(x,y) \\
\dot{E} &= (T-D)V/mg \\
\dot{h} &= V\sin\gamma \\
\dot{\gamma} &= (L\cos\phi - mg\cos\gamma)/mV \\
\dot{\varphi} &= L\sin\phi/mV\cos\gamma \\
\dot{m} &= -\sigma(h,V,T)
\end{aligned} \qquad (1)
$$

where x is the downrange position, y is the cross track position, E is the energy height, h is the altitude, γ is the flight path angle, ϕ is the roll angle, φ is the heading angle, m is the aircraft mass, T is the aircraft thrust, D is the drag and V is the airspeed. The fuel flow σ is a function of thrust, altitude and air speed. *u(x, y)* and *v(x, y)* are the x- and y-components of the wind.

3.2 Atmospheric Models

Rapid Update Cycle (RUC), an operational weather prediction system developed by NOAA for users needing frequently updated short-range weather forecasts (e.g. US aviation community), provides the wind, temperature and humidity used in the atmospheric models [6]. RUC provides wind and other atmospheric parameters in a grid using Lambert conformal conic projection coordinates. The grid is rectangular on this projection. The horizontal resolution in RUC varies from 40.6 km at 35 degrees N to 38 km at 43 degrees N and has an average grid size of 40-km. RUC data has 37 vertical isobaric pressure levels ranging between 100-1000 hPa in 25 hPa increments. Lambert coordinates can be easily converted into spherical coordinates using latitude and longitude using trigonometric formulas. RUC data is updated every hour and provides current wind, temperature, humidity and other atmospheric parameters and forecast of these parameters for the next 5 to 6 hours. The 40-km RUC data can be represented as a three-dimensional matrix $R(I,J,K)$, where I=1,..113, J=1,..151, and K=1,..11, corresponding to the eleven pressure altitudes from 400 hPa to 150 hPa. The altitude level index K and the corresponding pressure level and flight level are listed in Table 1. As an example, snap shots of temperature and relative humidity with respect to water (RHw) contours at 8AM eastern daylight time (EDT) on August 1, 2007 at pressure altitude 250 hPa, or 34,057 feet, are shown in Fig. 2.

Table 1. Altitude level index, isobaric pressure level, and flight level.

Level index	pressure level (hPa)	flight level (100 feet)
1	400	236
2	375	251
3	350	267
4	325	283
5	300	301
6	275	320
7	250	341
8	225	363
9	200	387
10	175	414
11	150	444

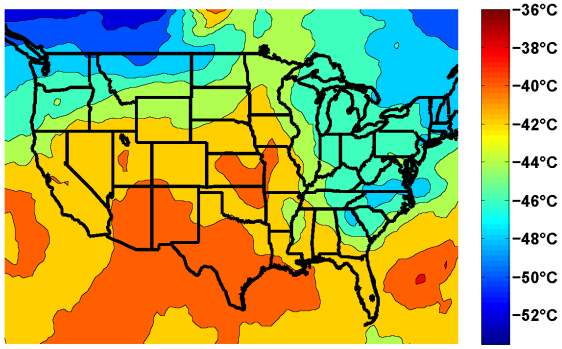

(a) Temperature

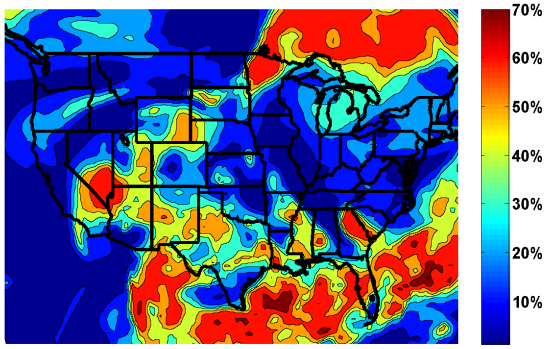

(b) Relative humidity with respect to water

Fig 2. Contours of temperature and RHw at 250 hPa at 8AM (EDT) on August 1, 2007.

3.3 Fuel flow and emission

This study uses the fuel consumption model developed for the FAA Aviation Environmental Design Tool [7] to compute cruising aircraft fuel consumption. This model refines Eurocontrol's Base of Aircraft DAta Revision 3.6 (BADA) [8] by taking into account the

variability of engine performance with meteorological conditions and throttle setting. The specific fuel consumption can be expressed as a function of Mach number, pressure, and aircraft related parameters. The following equation calculates fuel burn for aircraft during cruise

$$f = t \cdot SFC \cdot T, \qquad (2)$$

where f is the fuel burn, t is elapsed time, T is thrust, and SFC is the specific fuel consumption.

3.4 Contrails

3.4.1 Contrail formation model

The formation of contrails has been under investigation since 1919 [9]. According to Appleman [10], contrails are clouds that form when a mixture of warm engine exhaust gases and cold ambient air reaches saturation with respect to water, forming liquid drops, which quickly freeze. Contrails can persist when the ambient air is supersaturated with respect to ice i.e. the environmental relative humidity with respect to ice (RHi) is greater than 100% [11]. In this study, the regions of airspace that have RHi greater than 100% are considered favorable to persistent contrails formation.

The RHi is computed using measurements from the Rapid Update Cycle (RUC). RUC does not provide measurements for RHi directly. Instead, it has measurements for Relative Humidity with respect to water (RHw) and environmental temperatures. They are used to compute the RHi by the following formula,

$$RHi = RHw \cdot \frac{6.0612 e^{18.102 \cdot T/(249.52+T)}}{6.1162 e^{22.577 \cdot T/(273.78+T)}} \qquad (3)$$

where T is temperature measured in Celsius. The numerator on the right hand side of Eq. (3) represents the saturation vapor pressure over water and vapor pressure over ice [12].

Using Eq. (3) and the RUC data [11], it is possible to create a three-dimensional matrix $P(I,J,K)$ with zeros and ones indicating grid points where the conditions are unsuitable or suitable for contrail formation. Further, the RUC forecast permits the computation of predicted values of $P(I,J,K)$ for the next six hours.

The continental United States is divided into twenty centers for air traffic operations. The potential persistent contrail coverage ratio of one center can be defined by the total of the contrail areas divided by the area of the center. As an example, the contrail area at flight level 341 at 8AM (EDT) on August 1, 2007 is shown in Fig. 3a. The corresponding center contrail coverage ratio is shown in Fig. 3b. The center contrail coverage ratio provides information whether contrail reduction is needed. In general, when the ratio is small, no action is needed. When the ratio is high, contrail reduction strategies may be needed.

Persistent contrails can spread through the atmosphere due to winds to form cirrus-like clouds, which are indistinguishable from natural clouds. Another source of cloud formation is the particles containing black carbon, sulphate and organic compounds emitted by aircraft engines at cruise altitudes. The accumulation of these particles may act as nuclei for the formation of clouds. There have been studies to measure the validity of contrails formation by comparing them with satellite observation [13-14].

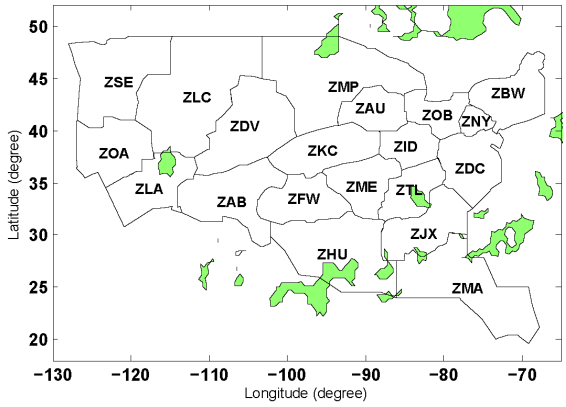

(a) Potential persistent contrail formation area

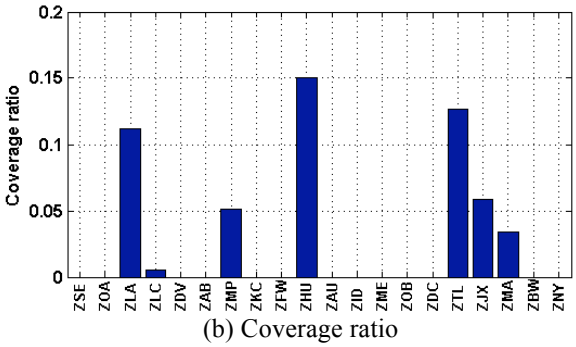

(b) Coverage ratio

Fig 3. Potential persistent contrail formation area and coverage ratio at flight level 341 at 8AM (EDT) on August 1, 2007.

3.4.2 Frequency Index

The contrail formation model provides regions satisfying the necessary conditions for contrail formation. Contrails form when aircraft fly through a potential contrail formation area. Therefore planned aircraft locations are needed to determine the contrail formation frequency. The contrail frequency index is a convolution of traffic data and atmospheric conditions similar to the concept of Weather Impacted Traffic Index (WITI) introduced by Callaham et al[15] and Sridhar [16] and the three dimensional index derived by Chen [17]. The aircraft data used in this paper were extracted from the Federal Aviation Administration's Aircraft Situation Display to Industry (ASDI) data. The ASDI has a sampling rate of one minute. The same geometry grid used in the RUC data was used to generate the aircraft position matrix. The aircraft position matrix, $A(I,J,K)$, is the number of aircraft within grid *(I,J)* flying closest to altitude level K at a given time t. The contrail frequency index, $CF(I,J,K)$, defined as the number of aircraft, flying through the potential contrail grid area at level K and is equal to

$$CF(I,J,K) = A(I,J,K) * P(I,J,K) \qquad (4)$$

As in the case of WITI, the index is affected more by the changing atmospheric conditions than by small daily variations to the nominal traffic plan.

The Contrail Frequency Index of Center L, *CFI(L,K)*, at altitude K is derived by summing it for all values of I and J which lie within the Center L.

As an example, the center contrail frequencies at flight level 341 were computed at 8AM (EDT) on August 1, 2007 and are shown in Fig. 4a. Even though the contrail coverage ratio of Houston Center (ZHU) is higher than Atlanta Center (ZTL), as seen in Fig. 3b, the contrail frequency of Houston Center is zero. Figure 4b and 4c show the aircraft locations and contrail areas of Houston and Atlanta Center. The small green dots indicate the aircraft trajectory. The contrail areas are shown in blue contours. The big red dots show the aircraft inside the contours, where persistent contrail occurs. As shown in the figures, Houston Center

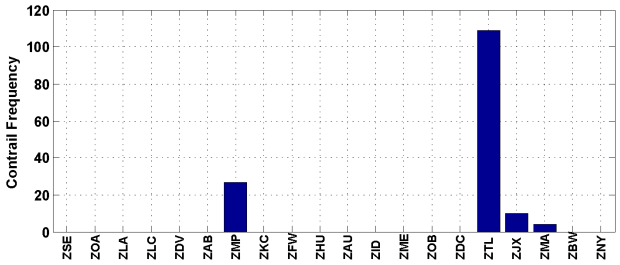

(a) Center contrail frequencies at flight level 341 at 8AM (EDT) on August 1, 2007

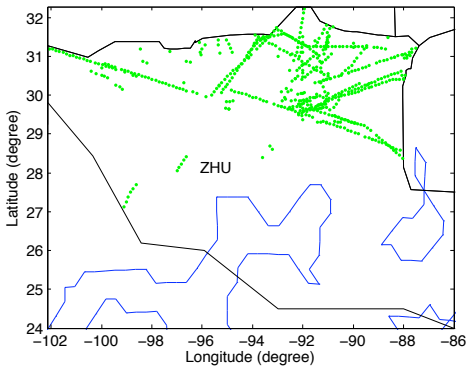

(b) Houston center, contrail frequency=0

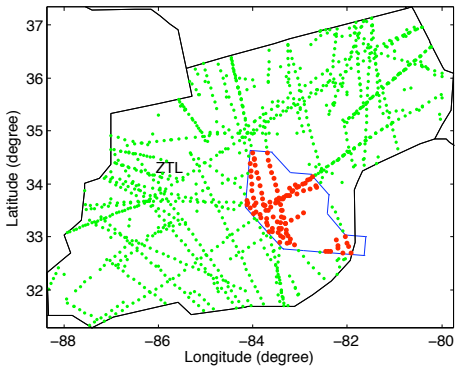

(c) Atlanta center, contrail frequency=142

Fig 4. Aircraft location and potential persistent contrail formation areas at 8AM (EDT) on August 1, 2007.

has larger contrail areas, but no aircraft flying through the contours, while there are more aircraft flying through the contours at Atlanta Center. The center contrail frequency is 0 in Houston Center and 109 in Atlanta Center. This example shows that the center contrail coverage ratio does not reflect the actual severity of contrail frequency in a center. The contrail frequency is a better indication of the severity of contrail formation.

3.4.3 Prediction

Initially the ability to predict CFI at a given altitude for durations of one, two, three and six hours at all the centers is considered. Figure 5a shows the actual and predicted center contrail

frequency indices at flight level 341 at 8AM (EDT) on August 3, 2007. The blue bars are the actual, and the other color bars are the one-hour, two-hour, three-hour, and six-hour predicted contrail frequency indices computed by Eq. (4) using traffic data on July 18, 2007. As shown in the figure, the actual and predicted contrail frequency indices are highly correlated. For example, at Jacksonville Center (ZJX), the actual contrail frequency index is 692. The one-hour, two-hour, and three-hour predicted indices are within 10% error. The six-hour predicted index has larger error, most likely due to the prediction accuracy of 6-hour RUC forecasts. For implementing contrail avoidance strategy, the centers with high contrail frequency indices need to be identified. As an example, the contrail avoidance strategy may be enabled when the centers have indices higher than 100. This would affect Minneapolis, Washington D.C. and Jacksonville Centers. All of the one-hour, two-hour, and three-hour prediction indices are able to correctly identify the centers that need a reduction strategy. The six-hour prediction identified Washington D.C. and Jacksonville Center, but failed to identify Minneapolis Center. There are also some errors in the six-hour prediction by falsely identifying center (Boston Center) with low contrail activity as having an index greater than 100. Overall the prediction indices provide a 95% success rate of identifying the correct centers.

Hourly predictions for the twenty continental U.S. center contrail formation frequencies were generated in August 2007. The one-hour, two-hour, three-hour, and six-hour predicted indices were also generated and analyzed. The predicted contrail frequency index was based on aircraft data of July 18, 2007. The actual and one-hour prediction contrail index at flight level 341 at Jacksonville Center is shown in Fig. 5b.

As shown in the figure, the one-hour predicted contrail index is highly correlated with the actual index, with a correlated coefficient of 0.97. The correlated coefficient between the actual index and the two-hour, three-hour, and six-hour predicted index are 0.84, 0.74, and 0.51, respectively. As noted earlier, the correlation coefficients are lower for

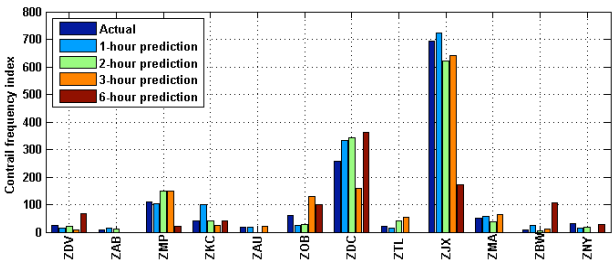

(a) Center contrail frequencies at flight level 341 at 8AM (EDT) on August 3, 2007

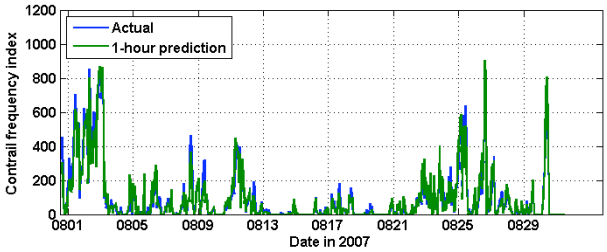

(b) Center contrail frequencies at flight level 341 at Jacksonville center in August 2007

Fig 5. Actual and predicted center contrail frequency index.

longer prediction period due to the prediction accuracy of RUC models. Similar trends are seen in all the other 19 centers [17]. The accuracy of the parameters provided by RUC varies with altitude. The humidity, RHW, is known to be underestimated at higher altitudes. The sensitivity of contrail regions can be computed with respect to errors in RUC parameters.

4 Contrail Avoidance Strategies

The selection of strategies for contrail avoidance should be based on several different considerations. Although avoiding contrails is similar to re-routing aircraft in the presence of severe weather, which is done for the safety of the aircraft and its passengers, contrail avoidance is preventive action taken to reduce the impact of aviation on climate. Thus, contrails can be treated as a soft constraint in the avoidance problem. Using CFI or other metrics, the area to be avoided can be made a function of the severity of contrail formation in a particular region. Generally, avoiding contrails may result in extra fuel consumption and the associated increase in CO_2 emissions. Even without addressing the questions relating to congestion and other ATM factors resulting from the reroutes, one has to balance the long-term effect

of extra CO_2 emissions with the short-term effect of going through potential contrail formation areas. Thus it is necessary to develop a flexible, either partial or complete, avoidance approach that can create several options for avoiding all or some of the potential contrail formation areas.

Several new operational strategies in air traffic management have been proposed that can potentially mitigate the impact of persistent contrails on climate change. These strategies include adjusting cruise altitude in real-time [18] and rerouting aircraft around region of airspace that facilitate persistent contrails formation [19]. The study in Ref. 20 presents a methodology to optimally reroute aircraft trajectories to avoid the formation of persistent contrails with the use of mixed integer programming. However, the computational complexity is very high for problems with many obstacles and dynamic constraints. None of the current methods for avoiding contrails [20-21] consider the effect of wind on the aircraft trajectory and neglect the potential fuel savings that aircraft can gain when flying wind-optimal routes.

The strategy for reducing the persistent contrail frequency in this paper is to minimize the overall environmental impact. Methods with minimum additional fuel utilization are preferred. The approach first selects a severity level for contrail formation. This determines contrail formation regions to avoid either partially or completely. Two different avoidance methods are used with one involving only altitude changes and another involving changes both to the altitude and route of the aircraft.

4.1 Altitude Changes

The predicted contrail frequency index is used to identify the potential centers and flight levels with high contrail frequency. The cruise altitudes of this group of aircraft is moved up using airspace above it, while air traffic density below airspace capacity. Consider Atlanta Center at 8AM (EDT) on August 1, 2007, the center predicted contrail frequency index at different altitudes is shown in Fig. 6a. The altitudes shown in Fig. 6a are based on the RUC grid and can be easily converted into standard flight levels. As suggested in the figure, flight level 341 has the highest frequency index, thus was chosen as the level to be avoided. Figure 6b shows the one-hour simulation of contrail formations at Atlanta Center at 8AM (EDT). The color lines indicate contrail areas at different altitudes. The color dots indicate the aircraft flying through the contrail areas. Different colors mean different altitudes, from blue at flight level 236, to red at 444. There are total 188 dots in the figure, which is the center contrail frequency at all flight levels. When the avoidance strategy was applied, all the aircraft flying at and above flight level 341 were moved up one level. The simulation result is shown in Fig. 6c.

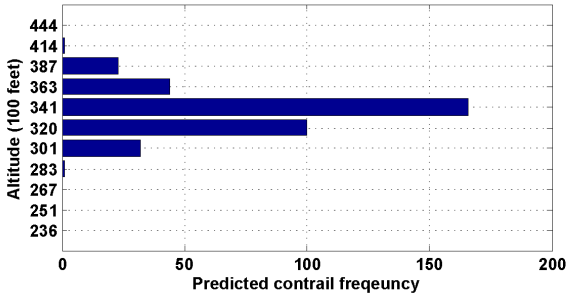

(a)) Predicted contrail frequency index

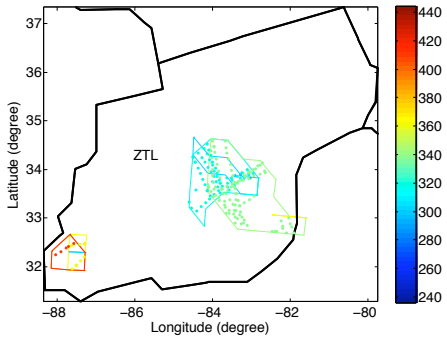

(b) without contrail reduction

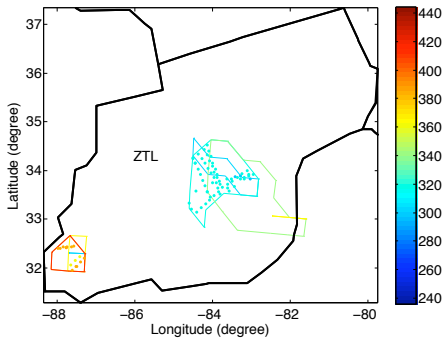

(c) with contrail reduction

Fig 6. Predicted contrail frequency index and potential contrail formation area, with and without contrail reduction action, at flight level 341 at 8AM (EDT) on August 1, 2007.

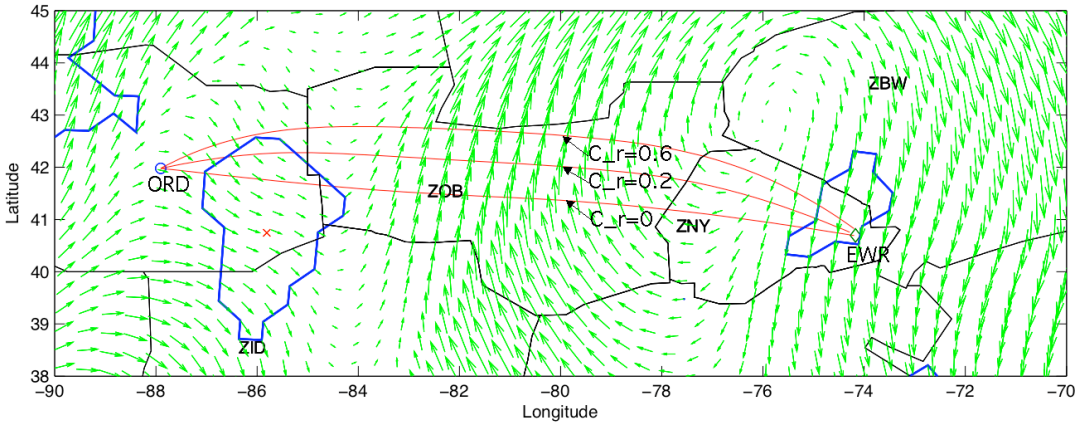

Fig 7. Optimal trajectories with different design parameters from ORD to EWR.

In the figure, all the light green dots disappear, which means that all the aircraft producing contrails at flight level 341 were eliminated. Since the contrail areas above fight level 341 were much smaller, the contrail frequencies were reduced. The total dots in the figure are 80. That is, with the avoidance strategy applied, the contrail formation frequency was reduced by 42.55%.

4.2 Optimal avoidance strategy

Aircraft trajectory optimization algorithms are well-known and are solutions to two-point boundary value problems [22]. The various approximations to the solution of the two-point boundary value problems depend on the application, and are motivated by the desire to balance computation speed with accuracy. The cruise altitude of most aircraft varies between 29,000 feet to 41,000ft. The flight levels are separated by 2000 feet between two levels of flight in the same direction (1000 feet since the introduction of Reduced Vertical Separation Minimums). As the choice of the cruise altitude varies over a small range, the optimal aircraft trajectories in this paper are computed by repeatedly solving the horizontal plane problem.

The equations of motion on the horizontal plane are

$$\begin{aligned} \dot{x} &= V\cos\varphi + u(x,y) \\ \dot{y} &= V\sin\varphi + v(x,y) \\ \dot{m} &= -f \end{aligned} \tag{5}$$

subject to the conditions that T=D and γ=0. The horizontal trajectory is optimized by determining the heading angle, φ, that minimizes a cost function and satisfies the physical system constraints. The cost function contains components that penalize travelling time, fuel burn, and flying through potential contrail formation area. The cost function is defined by

$$\begin{aligned} J = &\frac{1}{2}X^T(t_f)SX(t_f) \\ &+\int_{t_0}^{t_f}\left\{C_t + C_f f + C_r r(x,y)\right\}dt, \end{aligned} \tag{6}$$

where X is the state vector, $X(t_f)$ is the final state cost matrix, C_t is cost coefficient of time, C_f is cost coefficient of fuel, f is fuel consumption rate, C_r is cost coefficient of risk, and $r(x,y)$ is contrail formation area at a given altitude.

The application of optimal control theory results in a differential equation for φ. This section presents results based on applying the optimal trajectory algorithm [23] to calculate aircraft trajectory in the presence of winds that avoids regions of airspace that facilitate persistent contrail formation. The trade-off between fuel consumed and the amount of contrail avoidance is illustrated in terms of a flight from Chicago O'Hare Airport (ORD) to Newark Liberty Airport (EWR).

The blue polygons in Fig. 7 depict the potential contrail formation areas at 34,100 feet above sea level in the NAS at 6:00 a.m. EDT on May 24, 2007. Each polygon with a red cross is identified as a potential risk to the aircraft and the red-cross is the risk center. The position of

the risk centers and aircraft positions are used to calculate the distance and the risk. The green arrows represent the wind directions at 6 a.m. EDT based on RUC information. The arrow sizes are plotted in proportion to the wind magnitudes. The cruising speed is assumed to be 400 knots (741 km/hr) at an altitude of 34,100 feet. The wind-optimal trajectory from ORD to EWR is generated by ignoring the risk area with C_r=0. Two optimal trajectories in addition to the wind-optimal route are also plotted in Fig. 7. In this example, the cost coefficient of time is chosen as C_t=20 and the cost coefficients of risk are equal to 0.2 and 0.6, respectively. Note that the risk coefficient is treated as a design parameter. The choice of this parameter is not unique and depends on the definition of the risk itself. The optimal route, with C_r=0.6, completely avoids the contrail polygons near the departure airport. The optimal route, with C_r=0.2, only partially avoids the polygons but is shorter. Note that both routes travel through the green polygon surrounding the destination where aircraft start to land. In this case, there is a tradeoff between flying a shorter route with more persistent contrails formation versus flying a longer route with less persistent contrails formation.

The performance of optimal trajectories is evaluated by investigating the total travel time and the time associated traveling through regions of persistent contrails formation. Optimal aircraft trajectories are generated for ten different altitudes between 28,000 feet and 52,000 feet (i.e. corresponds to the isobaric pressure level between 325 hPa and 100 hPa with 25 hPa increments). Figure 8 shows the results for the ten wind-optimal trajectories. The sum of blue and red bars represents the total travel time for each trajectory, and the red bar presents the length of periods that a flight travels inside the regions of airspace favorable to persistent contrails formation. The wind-optimal trajectories at 28,300 ft, 41,400 ft, 44,400 ft, 47,800 ft and 51,900 ft do not intercept any region of airspace that facilitates persistent contrails formation. The flights at these cruising altitudes should fly the wind-optimal trajectories that minimize fuel burn and emissions. Flying wind optimal trajectories at other altitudes between 30,000 ft and 39,000 ft will potentially cause persistent contrails formation. Increasing the value of C_r from 0 to 2 with increments of 0.2 generates optimal contrails-avoidance trajectories at these altitudes. The green column in Table 2 shows the value of C_r, the total travel time for the contrails-avoidance trajectory and the additional travel time compared to that of wind-optimal trajectory. The blue bars show the travel time for wind-optimal trajectories. The additional travel times ranged from 0 to 4.3 %. Flying contrails-avoidance trajectory requires very small additional travel time at 38,700 feet, and that avoids potentially three minutes of persistent contrails formation. Flying contrails-avoidance trajectory at 34,100 feet requires 4.3 % more travel time to avoid forming potentially 16 minutes of persistent contrails. More optimal trajectories can be calculated with various choice of C_r. The optimal trajectory that minimizes climate change can then be determined when the relative severity of contrails and emissions on climate impact is known. An alternative strategy for the cruising flights to minimize climate impact can be altering the cruising altitude from 34,100 feet to the neighboring altitudes depending on the air traffic conditions. Generating and comparing these optimal trajectories at different flight altitudes provides policy-makers the necessary data to make tradeoffs between persistent contrails mitigation and fuel consumption. A more detailed analysis of the optimal aircraft contrail avoidance trajectories is presented in [23].

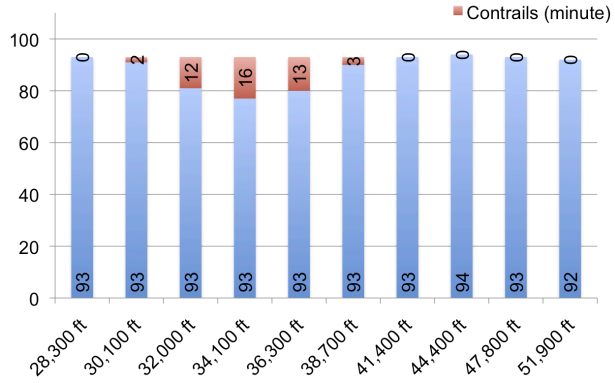

Fig. 8. Travel time for the wind-optimal routes from ORD to EWR and length of periods favorable to persistent contrails formation at 8 different altitudes.

Table 2. Wind-optimal trajectories versus contrails-avoidance trajectories from ORD to EWR.

Altitude (ft)	30,100		32,000		34,100		36,300		38,700	
C_r	0	0.4	0	1.6	0	0.6	0	1.8	0	0.2
Trajectory (minute)	93	94	93	95	93	97	93	95	93	93
Contrails (minute)	2	0	12	0	16	0	13	0	3	0
Additional Travelling Time (%)	0	1.1	0	2.2	0	4.3	0	2.2	0	0
Fuel Burn (kg)	3520	3560	3440	3510	3360	3510	3310	3380	3270	3270

5 Concluding Remarks

The planning of air traffic schedules is a multi-dimensional optimization problem involving trade-offs between safety, capacity and efficiency. The recognition of the impact of aviation on the environment, together with the uncertainties associated with it, requires simulation and optimization tools to generate best operations policies towards sustainable aviation. This paper discusses some of the modeling, simulation and optimization issues associated with the problem. The contributions of the paper are (a) introduction of the concept of contrail frequency index, (b) prediction of the index using atmospheric data and (c) two methods for avoiding contrails that provide a trade-off between avoiding contrails (e.g., by reducing the contrail frequency index) and the amount of extra fuel consumption. The three-dimensional avoidance methodology is illustrated with a flight originating in Chicago and heading to Newark. Additional results about the three-dimensional approach and the altitude-only approach are presented in two companion papers [17,23]. The software structure and the preliminary results presented in the paper can be used as building blocks for a more in-depth study of the impact of aviation on the environment.

References

[1] Aviation and the global atmosphere, intergovernmental panel on climate change. Cambridge University Press, Cambridge, UK, 1999.

[2] NASA workshop on the impacts of aviation on climate change. June 7-9, 2006, Boston, MA.

[3] Bilimoria K, Sridhar B, Chatterji G, Sheth K and Grabbe S. FACET: future ATM concepts evaluation tool. *Air Traffic Control Quarterly*, Vol. 9, No. 1, 2001.

[4] Grabbe S, Sridhar B, and Mukherjee A. Sequential traffic flow optimization with tactical flight control heuristics. *AIAA Journal of Guidance, Control and Dynamics*, Vol. 32, No. 3, pp. 810-820, 2009.

[5] Sridhar B, Grabbe S and Mukjerjee A. Modeling and Optimization in Traffic Flow Management. *IEEE Proceedings*, January 2009.

[6] Benjamin S G, Devenyi D, Weygandt S S, Brundage K J, Brown J M, Grell G A, Kim D, Schwartz B E, Smirnova T G, Smith T L and Manikin G S. An hourly assimilation-forecast cycle: the RUC. *Monthly Weather Review*, Vol. 132, No. 2, 495-518, February 2004.

[7] Senzig D, Fleming G and Iovinelli R. Fuel consumption modeling in support of ATM environmental decision-making. *8th USA/Europe Air Traffic Management R&D Seminar*, Napa, CA, June-July, 2009.

[8] Eurocontrol experimental center (EEC). User manual for the base of aircraft data (BADA), revision 3.6. EEC note No. 10/04. Project ACE-C-E2. September 2004.

[9] Schumann, U. On conditions for contrail formation from aircraft exhausts. *Meteor. Z.,* **N. F. 5,** 3–22, 1996

[10] Appleman H. The formation of exhaust condensation trails by jet aircraft. *Bull. Amer. Meteor. Soc.,* **34,** 14–20, 1953.

[11] Duda D, Minnis P, Costulis P and Palikonda R. CONUS contrail frequency estimated from RUC and flight track data. *European Conference on Aviation, Atmosphere, and Climate*, Friedrichschafen at Lake Constance, Germany, June-July, 2003.

[12] Alduchov O A and Eskridge R E. Improved magnus form approximation of saturation vapor pressure. *Journal of Applied Meteorology*, Vol. 35, 601-609.

[13] Degrand J Q, Carleton A M, Travis D J and Lamb P J. A satellite-based climate description of jet aircraft contrails and associations with atmospheric conditions, 1977-79. *Journal of Applied Meteorology*, Vol. 39, pp. 1434-1459.

[14] Palikonda R, Minnis P, Duda D P and Mannstein H. Contrail coverage derived from 2001 AVHRR data over the continental United States of America and surrounding areas. *Meteorologische Zeitschrift*, Vol. 14, No. 4, 525-536, August 2005.

[15] Callaham M B, DeArmon J S, Cooper A, Goodfriend J H, Moch-Mooney D and Solomos G. Assessing NAS performance: normalizing for the effects of weather. *4th USA/Europe Air Traffic Management R&D Symposium*, Santa Fe, NM, December 2001.

[16] Sridhar B and Swei S. Relationship between weather, traffic and delay based on empirical methods. *6th AIAA Aviation Technology, Integration and*

Operations Conference (ATIO), Wichita, KS, September 2006.

[17] Chen N, Sridhar B and Ng H K. Strategies for reducing contrail formations using predicted contrail frequency index. *AIAA Guidance, Navigation, and Control Conference*, Toronto, Canada, 2010.

[18] Klima K. Assessment of a global contrail modeling method and operational strategies for contrail mitigation. M.S.Thesis, MIT, 2005.

[19] Mannstein H, Spichtinger P and Gierens K. A note on how to avoid contrail cirrus. *Transportation Research Part D*, Vol. 10, No. 5, 2005, pp. 421-426.

[20] Campbell S E, Neogi N A and Bragg M B. An optimal strategy for persistent contrail avoidance. *AIAA Guidance, Navigation, and Control Conference*, Honolulu, Hawaii, 2008.

[21] Gierens K, Lim L and Eleftheratos K. A review of various strategies for contrail avoidance. *The Open Atmosphere Science Journal*, 2, 1-7, 2008.

[22] Bryson, A E and Ho Y C. *Applied Optimal Control*. Taylor and Francis, Levittown, PA, 1975.

[23] Sridhar B, Ng H K and Chen N. Aircraft trajectory optimization and contrails avoidance in the presence of winds. *AIAA Aviation Technology, Integration, and Operation Conference*, Fort Worth, TX, 2010.

6 Contact Author Email Address

Banavar.Sridhar@nasa.gov

Copyright Statement